Finite Volume Calculation of Three-Dimensional Potential Flow Around a Propeller

Wen-Huei Jou*
Flow Industries, Inc., Kent, Washington

The development of a finite volume scheme for computing potential flow around a rotating propeller is presented. First, the governing potential equations are derived. General mesh properties, as well as the method of mesh generation, are discussed. Solution of the Mach 0.6 flow around an SR1 propeller is given. Near the leading edge, a low-density region terminated by a strong shock wave is indicated. The result is further confirmed by two-dimensional calculations of the airfoil section. At Mach 0.8, the calculation diverges with an indication of a separated cavity near the leading edge. The ability of the code to compute a high-speed flow is demonstrated by the calculation of Mach 0.8 flow around a fictitious propeller with an NACA 0012 cross section. A physical picture of a two-scale flowfield is conjectured for high-speed flow around a blade with a sharp leading edge. With the assumption that the local leading-edge flow does not affect the global flow, a solution of Mach 0.8 flow around an SR1 propeller can be obtained.

Introduction

THE continued high cost of airplane fuel has stimulated research toward developing an energy-efficient transport airplane. One of the programs along this line is the development of an advanced technology turboprop. Conservative estimates have put the potential fuel savings at between 14 and 30% of the consumption of current transport aircraft. An advanced turboprop typically operates at Mach 0.8, with an advance ratio of approximately 3. This combination gives a tip Mach number of around 1.2. Many technical problems arise from this high tip speed, one of which is the evaluation of aerodynamic performance. An advanced propeller usually consists of eight to ten blades, each blade highly swept and highly twisted with a small aspect ratio. The aerodynamics of flow around such a propeller at high speeds can be exceedingly complex.

The earliest work on propeller aerodynamics was the classical paper by Goldstein.[1] He investigated the induced flow by the helical vortex wake for incompressible flow. An optimum load distribution along the blade was then obtained. Incompressible lifting line theory for the wing has recently been extended in order to compute flows around a propeller. These methods are reviewed by Bober and Mitchell.[2] Attempts are made to take into account the flow induced by the hub and the effect of a curved blade in an ad hoc manner. The earliest known work on compressibility effects on a high-speed propeller was by Busemann.[3] Within the framework of linearized theory, he decomposed the velocity potential into Fourier-Bessel components and noted changes in the characteristics of the solution across the "sonic circle." The Fourier-Bessel representation of the solution was used to illuminate possible acoustic resonance when testing a high-speed propeller in a wind tunnel. Davidson was probably the first to compute quantitatively the effect of compressibility in a lifting line theory.[4] Specific computation was made for a propeller operating at an advance Mach number of 0.8193 with an advance ratio equal to π. His results showed that the compressibility effect contributes only 2% of the induced flow angle at the lifting line. These results were all obtained under the assumption of a high aspect ratio, so that the idea of a lifting line is applicable. Recently, Hanson has reported results obtained by using a lifting surface analysis in which a fundamental solution from a lifting element in a high-speed helical flow is used to construct the global solution that satisfies boundary conditions on the blade surface.[5] It is a linear theory which neglects the thickness of the blade, however.

In the past ten years, the numerical solutions of potential flow around a three-dimensional complex geometry have been developed to a high degree of sophistication. They are routinely performed in the aerodynamic designing of the wing. The methodology used there should be applicable to the present problem. The nonlinear governing equation and the exact boundary conditions, as well as the effects of complex geometry such as the hub-induced flow and cascade effects, can be included in the computations.

This paper presents the preliminary results of an attempt to apply the finite volume scheme of Jameson and Caughey for potential flow calculations to this problem.[6] A brief derivation of governing equations will be given, followed by a discussion of methods of grid generation for the present problem. Numerical methods and some preliminary results are also presented. Finally, a discussion of the possible physical mechanism that may have played an important role in the aerodynamics of the propeller is given.

Governing Equations

The flowfield around a rotating propeller is in a steady state if it is observed in a blade-fixed coordinate system. If the viscous effects are confined in a thin layer adjacent to the solid surface, the flow is governed by an inviscid equation of motion. Furthermore, if the flow is unsteady but irrotational in the nonrotating frame of reference, it must be governed by a potential equation in the blade-fixed frame, despite the artificially imposed rigid body rotation in a rotating frame. Derivations of the potential equation in a rotating frame are available from the literature by transforming the equations from an unsteady form in the nonrotating frame to those in the rotating frames through direct chain-rule substitutions (e.g., Caradonna[7]). In the following, we offer a concise derivation based on the steady-state Euler equation in a rotating frame. This derivation is not only simple, but it also provides better physical insight into the problem.

The steady-state Euler equation under a homentropic assumption in a coordinate system rotating with angular

Presented as Paper 82-0957 at the AIAA/ASME Third Joint Thermophysics, Fluids, Plasma and Heat Transfer Conference, St. Louis, Mo., June 7-11, 1982; submitted June 25, 1982; revision received Dec. 3, 1982.

*Senior Research Scientist, Research and Technology Division. Member AIAA.

velocity Ω can be given as

$$\nabla\left[\int\frac{dp}{\rho}+\frac{1}{2}q\cdot q-(\Omega\times r)\cdot(\Omega\times r)\right]-q\times(\omega+2\Omega)=0 \quad (1)$$

where q is the velocity vector, ω the vorticity vector, p the pressure, and ρ the density. A simple curl operation on this equation reduces it to the following vorticity equation.

$$q\cdot\nabla(\omega+2\Omega)=(\omega+2\Omega)\cdot\nabla q \quad (2)$$

The quantity $\omega+2\Omega$ is the absolute vorticity, as observed in a Newtonian frame. As expected from the physics of the flow, the absolute vorticity will be zero throughout the entire flowfield except on isolated vortex sheets if it is zero far upstream. If U_∞ is the advance velocity of the propeller, and r is the position vector, a perturbation velocity u', defined as

$$u'=q-(U_\infty+r\times\Omega) \quad (3)$$

can be shown to be irrotational, i.e.,

$$u'=\nabla\phi \quad (4)$$

where ϕ is the perturbation velocity potential, by using the condition of zero absolute vorticity. The conservation of mass can be shown as

$$\nabla\cdot[\rho(U_\infty+r\times\Omega+\nabla\phi)]=0 \quad (5)$$

Now, a relation between the density ρ and the perturbation velocity potential must be derived. This can be achieved by multiplying the Euler equation by the velocity. By using the irrotational relation (4) and the isentropic relation between pressure and density, the following form of Bernoulli's equation can be derived.

$$\frac{\rho}{\rho_\infty}=\left\{1-\frac{\gamma-1}{a_\infty^2}\left[(U_\infty+r\times\Omega)\cdot\nabla\phi+\frac{1}{2}\nabla\phi\cdot\nabla\phi\right]\right\}^{\frac{1}{\gamma-1}} \quad (6)$$

where γ is the ratio of specific heats and a_∞ is the speed of sound at infinity. If the density ρ is eliminated from Eqs. (5) and (6), the result is a nonlinear equation governing the perturbation velocity potential ϕ. These equations will be solved by a finite volume algorithm.

Mesh Generation

The first step of a finite volume calculation is to generate a computational mesh. The detailed considerations of mesh generation have been published earlier.[8] Here we shall briefly summarize some of the considerations of the mesh system, and the method of generating a desirable mesh system will be described.

The flowfield of a rotating propeller is periodic in the blade-to-blade direction. A natural choice for the computational mesh is a composite of two-dimensional meshes on a series of cylindrical-type surfaces intersecting the propeller blades. For this purpose, the hub-blade combination is augmented by a small-radius cylinder at the nose and a fictitious blade platform beyond the blade tip. The detailed considerations in augmenting the configuration have been discussed and will not be repeated here.[8] On these cylindrical-type surfaces, cross sections of blades form a cascade configuration, and two-dimensional cascade meshes will be generated. Two-dimensional meshes are divided into three categories: O-type, C-type, and H-type. The O-type meshes wrap around the entire blade cross section, while C-type meshes wrap around the leading edge and are open in the downstream direction. Both of these types of meshes have been successfully applied to two-dimensional calculations.[9] However, when a C-type mesh is applied to the three-dimensional calculations for the propeller problem, several difficulties arise. The upstream extent of the C-type mesh is of the order of the blade-to-blade spacing. For an eight-blade propeller, this spacing is less than a chord near the hub surface. With an axisymmetrical hub extending quite a distance upstream, however, the C-type mesh cannot adequately cover the hub surface, and the freestream condition is applied too close to the configuration. In addition, the trailing edge must be on a mesh line, i.e., the trailing-edge index must maintain constants along the span of the blade. Since the blade is highly twisted, the cascade configuration varies substantially along the span. If a set of trailing-edge indices is chosen, the resulting two-dimensional cascade meshes have unevenly distributed mesh spacing on the blade surface: very dense on the upper surface and sparse on the lower surface on the spanwise stations near the blade tip. Furthermore, on the surfaces beyond the blade tip, an internal artificially created boundary, i.e., the augmented blade platform, is present. The dense mesh on one side and the sparse mesh on the other require interpolation of the velocity potential across this fictitious boundary. Since the local undisturbed flow can be supersonic, the error of interpolation may create an undesirable mass source, which may cause the divergence of the solution.

An H-type mesh can be extended arbitrarily upstream and downstream. The blade cross section is mapped to an internal branch cut on which mesh spacing can be controlled. On the spanwise stations beyond the tip, there is no internal artificial boundary. It seems to be a better choice for the present complex configuration.

The following simple procedure is used to generate H-type meshes for the present problem.

1) Taking an isolated airfoil with a given leading-edge curvature, κ, the following transformation maps the branch cut along the positive real axis of the ξ plane to a parabola with the same curvature at the origin.

$$Z=i\xi^{1/2}+k\xi \quad (7)$$

2) By a simple shearing transformation, the parabola is sheared to the airfoil surface, while a pair of lines that coincide with the periodic boundary far upstream are sheared to two straight lines.

3) The transformed space, ξ, is divided into rectangular grids. The corresponding grid in the physical space is an H-type wind tunnel grid.

4) The resulting mesh is not periodic in the blade-to-blade direction. By a shearing transformation again, the meshes are distorted to satisfy the periodic boundary conditions.

Figures 1-3 show the resulting cascade meshes. These meshes are then sheared in the radial direction to make them conform to the axisymmetric hub.

Numerical Calculations

The finite volume algorithm of Jameson and Caughey[6] is used for computing the perturbation potential ϕ. The nonuniform undisturbed flow is computed at the center of

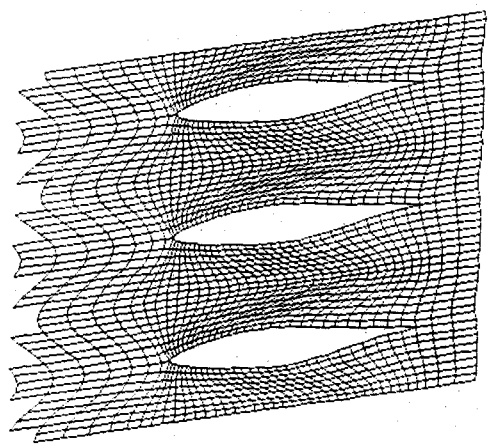

Fig. 1 Cascade mesh for SR1 blade, hub station.

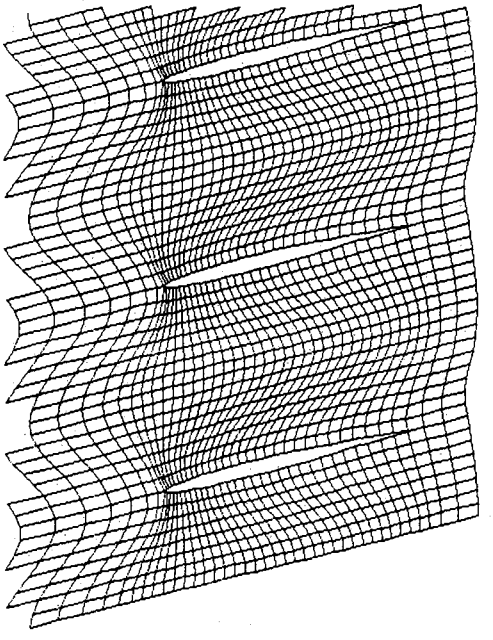

Fig. 2 Cascade mesh for SR1 blade, station near hub.

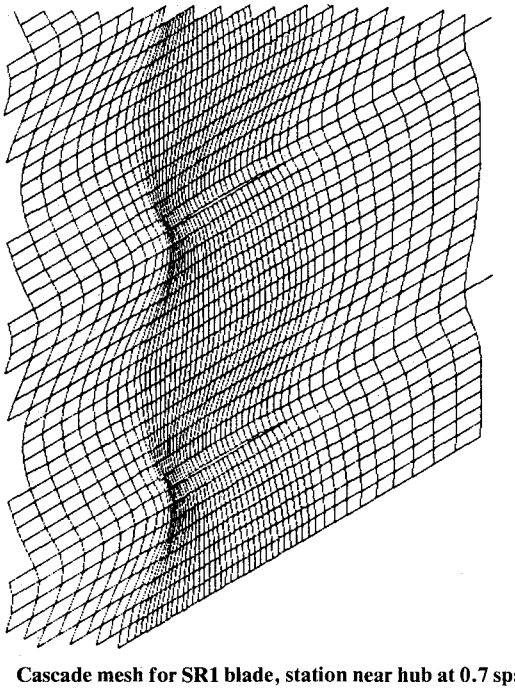

Fig. 3 Cascade mesh for SR1 blade, station near hub at 0.7 span.

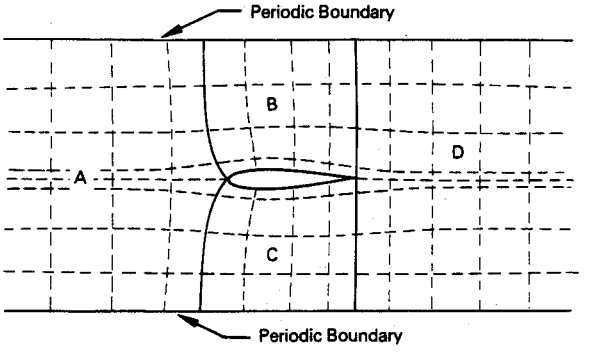

Fig. 4 Vertical line relaxation.

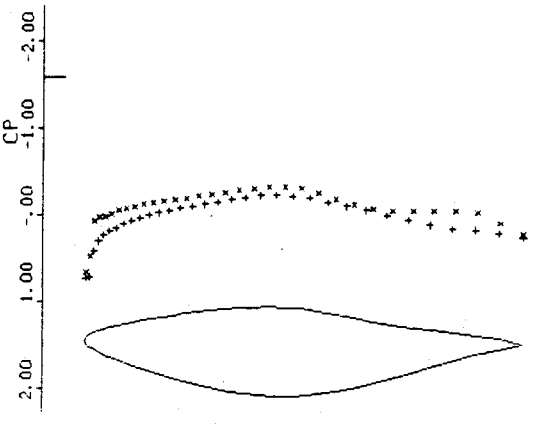

Fig. 5 Pressure distribution on SR1 blade at Mach 0.6, hub station.

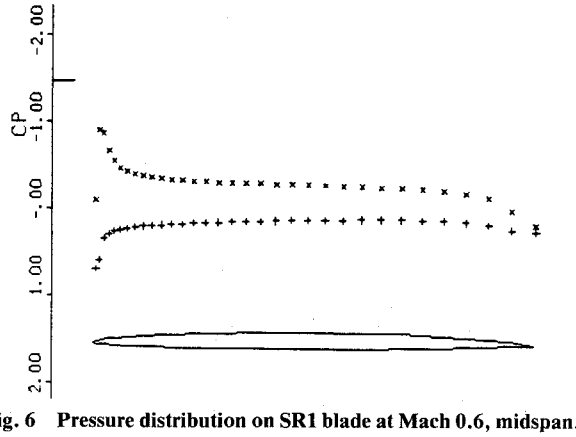

Fig. 6 Pressure distribution on SR1 blade at Mach 0.6, midspan.

each cell and the perturbation velocity is superimposed. Flux balance of the secondary cell can then be formulated using the computed velocity together with the proper density expression Eq. (6). Vertical line relaxation is used. Referring to Fig. 4, the potential along a vertical line is updated simultaneously in region A. In regions B and C, the lines start from the blade surface and end at the periodic boundaries. In region D, the potential along a vertical line is again updated simultaneously, but with the proper potential jump across the vortex wake subtracted out when computing the flux balance across the wake.

The sweeping direction is at a substantial deviation from the undisturbed flow off the tip of the blade. Because the flow is supersonic there, a substantial amount of artificial time damping must be added. In fact, the amount of the damping is scaled to the sixth power of the local Mach number to obtain a converging solution.

On the portion of the upstream boundary where the local undisturbed flow is supersonic, the Cauchy data are applied. On the downstream boundary, extrapolation of the velocity potential along the undisturbed flow direction has proven to be useful. Application of a nonreflecting condition on the outer cylindrical boundary has not been attempted for this preliminary calculation. The perturbation potential is given a zero value there.

Flows around an SR1 propeller† with a given axisymmetric hub are now computed. At the low advance Mach number of 0.6 with an advance ratio of 3.06 and twist angle at three-quarter span of 58 deg, the pressure distributions on the blade at several spanwise stations are shown in Figs. 5-7, where C_P is defined by the tip rotating speed. At some stations near the tip, a low-density region develops near the leading edge. A

†The SR1 propeller is an eight-bladed propeller designed for cruising at Mach 0.8. Geometrical data for the propeller can be obtained from NASA Lewis Research Center.

strong shock wave terminating the low-density region is indicated. To confirm this phenomenon, we turn to a two-dimensional airfoil calculation. The FLO 26 code developed by Jameson is applied to the airfoil section near the tip. The airfoil has a 2% thickness ratio with a leading-edge radius of 0.1% of the chord. The code uses a C-type mesh, and the mesh spacing near the leading edge is adjusted to resolve the leading-edge radius. Figure 8 shows the resulting mesh near the leading edge. At the freestream Mach number of 0.6, the pressure distribution on the airfoil is shown in Fig. 9. Again, a low-density region terminated by a strong shock wave is indicated. If the Mach number distribution over the two-dimensional flowfield is examined, the extent of the supersonic region is very small. Any attempt to increase the freestream Mach number of 0.8 causes the solutions to diverge. The three-dimensional calculation of the SR1 propeller at the advance Mach number of 0.8 also diverges. To further confirm that the sharp leading edge is the cause of the difficulty, a fictitious propeller with the same platform as the SR1 with an NACA 0012 cross section is tested for calculation at Mach number 0.8. The calculation shows good convergence, and the resulting pressure distribution is shown in Figs. 10-12.

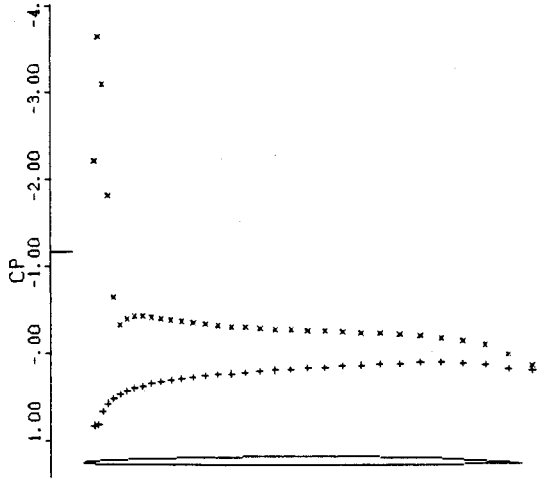

Fig. 7 Pressure distribution on SR1 blade at Mach 0.6, 0.84 span.

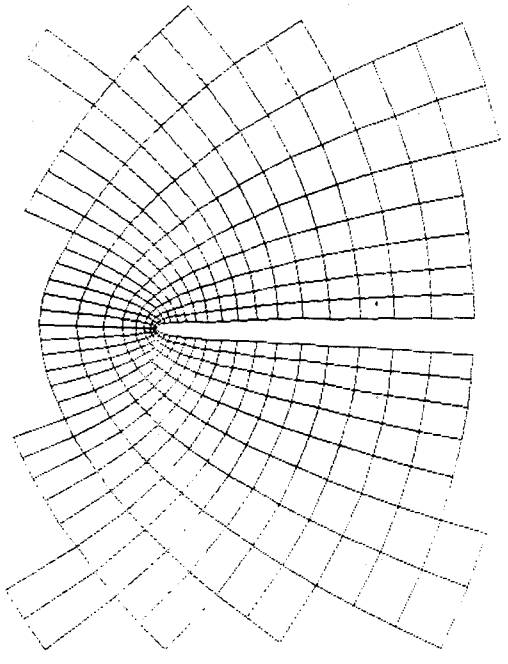

Fig. 8 Two-dimensional C-type mesh near leading edge of SR1 airfoil.

The physical picture seems to indicate that the flow is one with multiple scales. The outer flowfield in the global scale of the chord length determines the lift and, hence, the stagnation point. The local flow near the leading edge attempts to negotiate the small radius turn and expands to the limiting stream direction, leaving a zero-density bubble at the leading edge. This bubble is terminated by a strong shock wave on the upper surface. The local length scale is a function of Mach number, lift (angle of attack), and the leading-edge radius. A limiting case of a flat plate at the freestream Mach number 1.0 has been investigated by Vincenti et al.[10] A zero-density bubble terminated by a strong shock wave was shown in the framework of inviscid theory. The real flow can be even more complicated. Since the limiting speed of the flow at zero density is a finite value, the local Reynolds number is small. The effect of viscosity cannot be neglected. This dissipation, together with a strong shock wave in the scale of local flow, creates a strong entropy layer which is convected downstream along the blade surface. This strongly rotational entropy layer may affect the global flow and modify the lift if the interaction is strong. If one assumes that the outer flow is not affected by the local leading-edge flow to the lowest order,

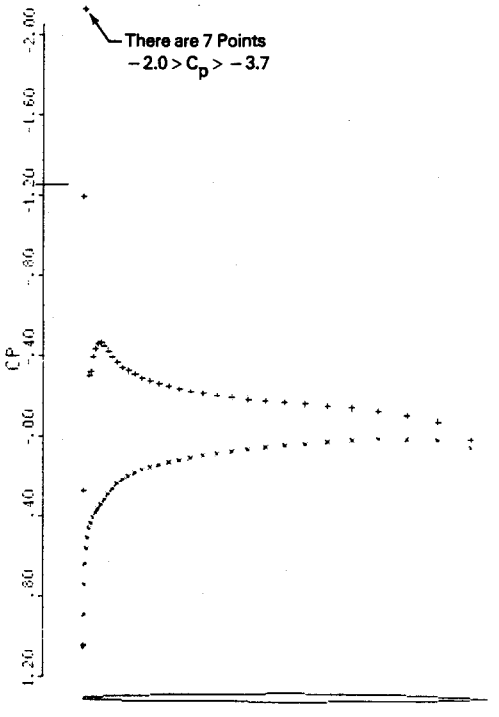

Fig. 9 Pressure distribution by two-dimensional calculation on SR1 airfoil at Mach 0.6 and an angle of attack of 2 deg.

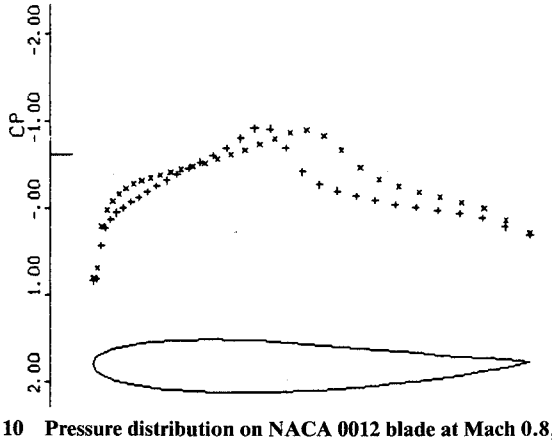

Fig. 10 Pressure distribution on NACA 0012 blade at Mach 0.8, hub station.

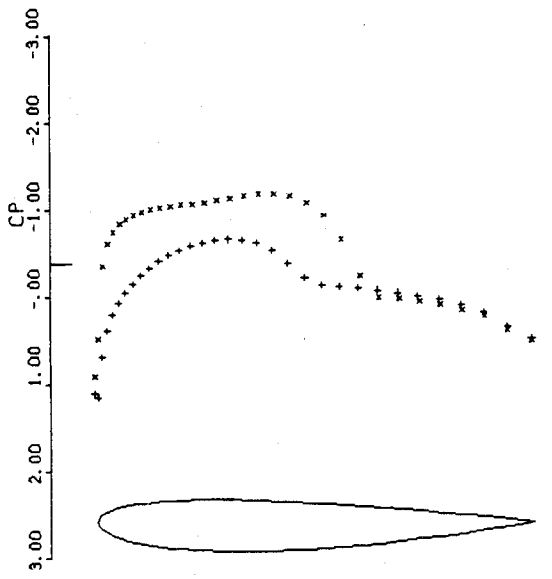

Fig. 11 Pressure distribution on NACA 0012 blade at Mach 0.8, 0.52 span.

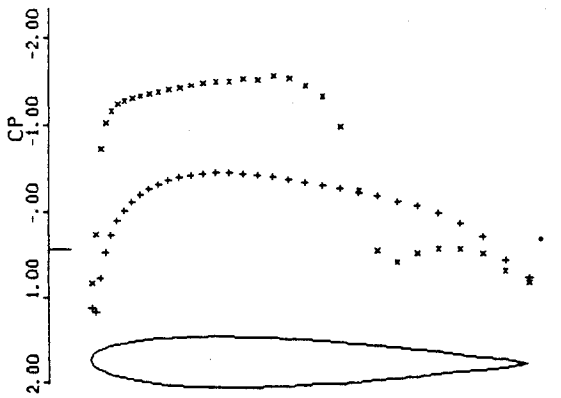

Fig. 12 Pressure distribution on NACA 0012 blade at Mach 0.8, 0.88 span.

one can intentionally adjust the mesh spacing near the leading edge so that the fast-varying local flow is averaged over the coarse mesh there. A converged solution can be obtained in this manner for a sharp leading-edge propeller, such as the SR1. The truncation error near the leading edge is very large; however, one hopes that this error is localized.

Conclusions

A finite volume code is developed for calculating flow around a rotating propeller at high speed. After some experimentation with the popular C-type mesh, it is concluded that an H-type mesh is more flexible for the present problem. An H-type mesh generated for the present problem is used successfully in the calculations. For propeller blades with a sharp leading edge, the calculation indicates that a low-density "bubble" develops very close to the leading edge. This low-density region is terminated by a strong shock wave. At high speeds, this fast expansion around the leading edge may leave a separated vacuum cavity within the inviscid theory. The existing finite volume calculation fails to give a converged solution for this case. However, a test calculation with a thick blade cross section shows that the present code is capable of computing the propeller flow at the advance Mach number 0.8. A physical picture can be conceived that consists of a local flowfield at the leading edge where the viscous effect is important and a strong but small shock wave is present. Away from this region, flow is governed by inviscid flow with a rotational entropy layer near the surface. The exact interaction of the local leading-edge flow and the global flow is not clear. If one assumes that the local leading-edge flow does not affect the global flowfield, the latter can be computed by using a mesh system constructed in the global scale. In this global mesh, the leading-edge flow is smoothed out and a converged solution can be obtained. The large truncation error at the leading edge is certainly recognized. Hopefully, the truncation error is localized to that area.

Acknowledgments

This work is supported by NASA Lewis Research Center under Contract NAS-22148. Discussions with Prof. Antony Jameson of Princeton University as well as Drs. Lawrence Bober and John Adamczyk of NASA Lewis Research Center have been helpful.

References

[1]Goldstein, S., "On the Vortex Theory of Screw Propellers," *Proceedings of the Royal Society (London)*, Series A, Vol. 123, No. 792, 1929.

[2]Bober, L. A. and Mitchell, G. A., "Summary of Advanced Methods for Predicting High Speed Propeller Performance," NACA TM-81409, 1980.

[3]Busemann, A., "Theory of the Propeller in Compressible Flow," presented at Third Midwestern Conference on Fluid Mechanics, Minneapolis, Minn., March 1953.

[4]Davidson, R. E., "Linearized Potential Theory of Propeller Induction in a Compressible Flow," NACA TN-2983, 1953.

[5]Hanson, D. B., "Compressible Lifting Surface Theory for Propeller Performance Calculation," AIAA Paper 82-0020, 1982.

[6]Jameson, A. and Caughey, D. A., "A Finite Volume Method for Transonic Potential Flow Calculations," *Proceedings of the Third AIAA Computational Fluid Dynamics Conference*, Albuquerque, N. Mex., 1977, pp. 35-54.

[7]Caradonna, F. X. and Isom, M. P., "Numerical Calculation of Unsteady Transonic Potential Flow over Helicopter Rotor Blades," *AIAA Journal*, Vol. 14, April 1976, pp. 482-488.

[8]Jou, W. H., "An Experience in Mesh Generation for Three-Dimensional Calculation of Potential Flow Around a Rotating Propeller," presented at Symposium on the Numerical Generation of Curvilinear Coordinate Systems, Nashville, Tenn., 1982.

[9]Jou, W. H., "Calculations of Transonic Potential Flow over Cascades," NASA CR 165471, 1981.

[10]Vincenti, W. G., Wagoner, C. B., and Fisher, N. H., "Calculations of the Flow over an Inclined Flat Plate at Free-Stream Mach Number 1," NACA TN-3723, 1956.